Available online at www.sciencedirect.com
ScienceDirect
NeuroToxicology 29 (2008) 428–443
NeuroToxicology

# Development of a physiologically based pharmacokinetic and pharmacodynamic model to determine dosimetry and cholinesterase inhibition for a binary mixture of chlorpyrifos and diazinon in the rat

C. Timchalk *, T.S. Poet

*Center for Biological Monitoring and Modeling, Battelle, Pacific Northwest Division, PO Box 999, Richland, WA 99352, USA*

Received 11 October 2007; accepted 8 February 2008
Available online 10 March 2008

**Abstract**

Physiologically based pharmacokinetic/pharmacodynamic (PBPK/PD) models have been developed for the organophosphorus (OP) insecticides chlorpyrifos (CPF) and diazinon (DZN). It is anticipated that these OPs could interact at a number of important metabolic steps including: CYP450 mediated activation/detoxification, B-esterases [carboxylesterase (CaE), butyrylcholinesterase (BuChE) and acetylcholinesterase (AChE)] or PON-1 (A-esterase) oxon detoxification. We developed a binary PBPK/PD model for CPF, DZN and their metabolites based on previously published models for the individual insecticides. The metabolic interactions (CYP450) between CPF and DZN were evaluated *in vitro* and suggests that CPF is more substantially metabolized to its oxon metabolite than DZN, which is consistent with observed *in vivo* potency (CPF > DZN). Each insecticide inhibited the other's *in vitro* metabolism in a concentration-dependent manner. The PBPK model code used to describe the metabolism of CPF and DZN was modified to reflect the type of CYP450 inhibition kinetics (i.e. competitive vs. non-competitive), while B-esterase metabolism was described as dose-additive, and no PON-1 interactions were assumed between CPF- and DZN-oxon with the enzyme. The binary model was then evaluated against previously published rodent dosimetry and cholinesterase (ChE) inhibition data for the mixture. The PBPK/PD model simulations of the acute oral exposure to single-mixtures (15 mg/kg) vs. binary-mixtures (15 + 15 mg/kg) of CFP and DZN resulted in no differences in the predicted pharmacokinetics of either the parent OPs or their respective metabolites, while cholinesterase inhibition was reasonably described using the dose-additive model. A binary oral dose of CPF + DZN (60 + 60 mg/kg) did result in observable changes in the DZN pharmacokinetics where $C_{max}$ was more reasonably fit by modifying the absorption parameters. It is anticipated that at low environmentally relevant binary doses, most likely to be encountered in occupational or environmental related exposures, that the pharmacokinetics are expected to be linear, and ChE inhibition dose-additive.


*Keywords:* Cholinesterase; Organophosphorus insecticide; Chlorpyrifos; Diazinon; Mixtures

## 1. Introduction

Organophosphorus (OP) insecticides like chlorpyrifos (CPF) (*O*,*O*-diethyl-*O*-[3,5,6-trichloro-2-pyridyl]-phosphorothioate) and diazinon (DZN) (*O*,*O*-diethyl-*O*-[2-isopropyl-4-methyl-6-pyrimidinyl]-phosphorothioate) have been extensively used for the control of agricultural and household pest. Exposure to these insecticides can involve a large segment of the population including, agriculture workers and their families, those living in proximity to farms/orchards, and the general population who may be exposed through home application of pesticides or via residues on food (Lu et al., 2000; Bradman et al., 2003; Quandt et al., 2004). Due to the variety of pesticides used, both occupational and environmental exposures are primarily to mixtures; however, only a few studies have begun to characterize the toxicological effects of exposures to concurrent or sequential OP pesticide mixtures (Marinovich et al., 1996; Karanth et al., 2001, 2004; Richardson et al., 2001; Abu-Quare et al., 2001; Moser et al., 2005, 2006; Timchalk et al., 2005).

The primary mechanism of action and the most life-threatening effect of these OP insecticides are related to the

* Corresponding author at: MSIN: P7-59, Battelle, Pacific Northwest Division, 902 Battelle, Boulevard, PO Box 999, Richland, WA 99352, USA. Tel.: +1 509 376 0434; fax: +1 509 376 9064.
*E-mail address:* charles.timchalk@pnl.gov (C. Timchalk).

0161-813X/$ – see front matter © 2008 Elsevier Inc. All rights reserved.
doi:10.1016/j.neuro.2008.02.004

accumulation of acetylcholine within the cholinergic synapses resulting from the inhibition of acetylcholinesterase (AChE). Based upon a shared common mechanism of toxicity (i.e. inhibition of AChE) (Mileson et al., 1998), the U.S. Environmental Protection Agency (EPA) under The Food Quality Protection Act (FQPA, 1996) is required to consider the cumulative risk associated with OP pesticide mixture exposures.

The metabolism of OP insecticides has been well studied (for review see, Chambers et al., 2001). In the case of CPF and DZN, metabolism to their active oxon metabolites involves CYP450-mediated oxidative desulfuration to CPF-oxon or DZN-oxon, whereas detoxification via CYP450-mediated dearylation produces TCP (3,5,6-trichloro-2-pyridinol) or IMHP (2-isopropyl-6-methyl-4-pyrimidinol), respectively (Fig. 1) (Sultatos and Murphy, 1983; Ma and Chambers, 1994, 1995; Amitai et al., 1998; Poet et al., 2003; Sams et al., 2000). The metabolism of CPF and DZN to their oxon metabolites is likely mediated by CYP 3A4, 2B6 (human), 2B1/2 (rat), and 2D6 (human) (Ma and Chambers, 1995; Sams et al., 2000; Tang et al., 2001). CYP-mediated dearylation resulting in the deactivation of CPF to TCP is likely mediated by CYP 2C and 3A4 (Tang et al., 2001). Hepatic and extra-hepatic PON-1 (A-esterase; *A-est*) can also effectively metabolize CPF- and DZN-oxon to TCP and IMHP without inactivating this esterase (Sultatos and Murphy, 1983). Whereas, B-esterases (*B-est*) such as carboxylesterase (CaE), butyrylcholinesterase (BuChE) and acetylcholinesterase (AChE) likewise detoxify the oxon metabolites; but these enzymes are subsequently inactivated (Chanda et al., 1997; Clement, 1984). Subsequent phase II conjugation of TCP and additional phase I oxidative metabolism of IMHP have also been reported in both humans and rodents exposed to CPF and DZN (Nolan et al., 1984; Mücke et al., 1970).

Richardson et al. (2001) suggested that the binary *in vitro* interactions of CPF-oxon and azinphos-methyl-oxon with brain AChE are best characterized using a dose-additive model, since the extent of AChE inhibition is dependent upon the relative potency of each oxon for the enzyme. In contrast, Karanth et al. (2001, 2004) reported that the sequence of exposure to OP insecticides dramatically influence the toxicological response. They reported that pre-exposure to CPF resulted in greater toxicity and ChE inhibition with sequential doses of parathion and methyl parathion, and concluded that CPF pretreatment effectively blocked the hepatic detoxification of paraoxon and methyl paraoxon (due to the depletion of CaE); whereas, the reverse (pretreatment with parathion and methyl parathion) had a minimal effect on the detoxification (PON-1 mediated metabolism) of CPF-oxon. Moser et al. (2005, 2006) evaluated a five-OP mixture (included CPF and DZN) for neurotoxicity interactions in adult and preweanling rats and evaluated the interaction using a fixed-ratio ray design where the pesticide doses were based on projected dietary exposure. Utilizing both neurochemical and behavioral endpoints they reported a greater than additive response when five OP insecticides were administered concurrently. These complex interactions for OP mixtures highlight the importance of chemical specific detoxification and suggest that a quantitative understanding of

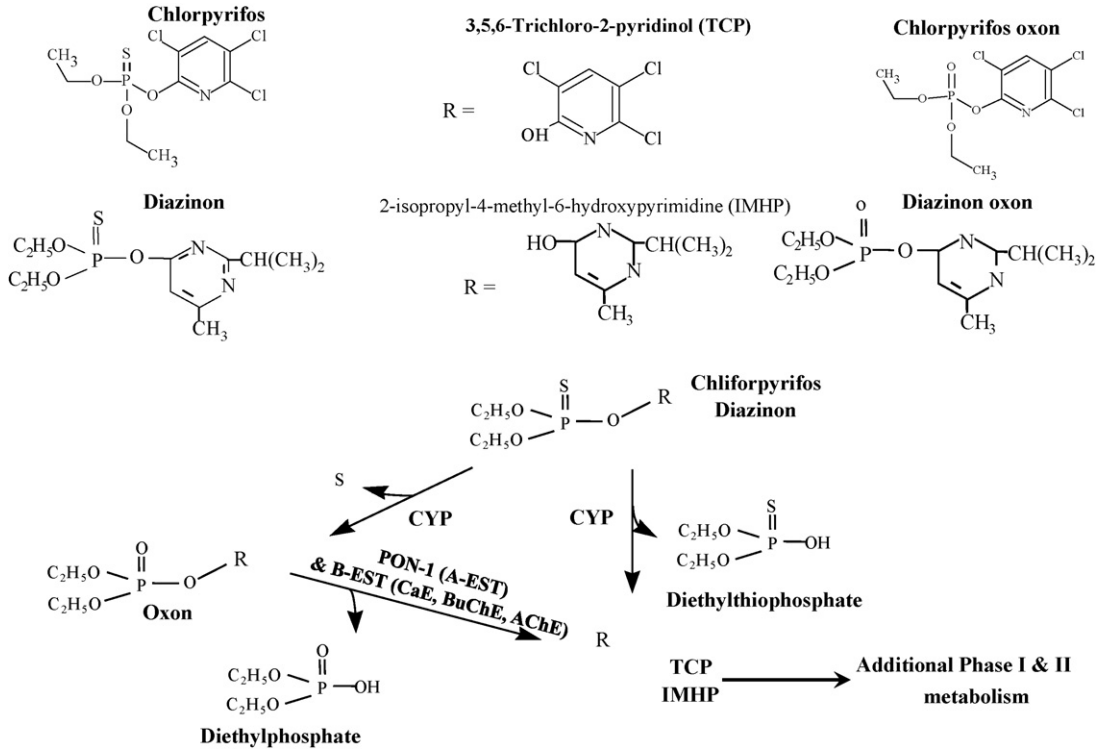


Fig. 1. Metabolic scheme for diazinon (DZN), chlorpyrifos (CPF) and their major metabolites (diazinon-oxon, 2-isopropyl-4-methyl-6-hydroxypyrimidine, chlorpyrifos-oxon, 3,5,6-trichloro-2-pyridinol, diethylphosphate and diethylthiophospate) showing the similarity in the metabolic profiles for both compounds.

metabolic interactions incorporated into a physiologically based pharmacokinetic/pharmacodynamic (PBPK/PD) modeling framework can provide important insight into mixture interactions.

The application of PBPK/PD modeling offers a unique opportunity to quantitatively assess cumulative biological response associated with binary-exposures to OP insecticide mixtures. Although PBPK/PD models for CPF or DZN in both rodents and humans have been developed (Poet et al., 2004; Timchalk et al., 2002), we are currently unaware of any published pharmacokinetic or pharmacodynamic models for binary mixtures of these insecticides. Based on similar pharmacokinetic and mode of action properties it is anticipated that OPs could interact at a number of important metabolic steps, including: oral absorption, CYP450 mediated activation/detoxification, PON-1 detoxification, protein binding, and blood/tissue cholinesterase (ChE) binding/inhibition. The net effect of these interactions (additivity, synergy or antagonism) will be dependent upon the specific OP mixture, exposure dose ranges and sensitivity of the individual.

This manuscript describes the development of a binary PBPK/PD model for CPF, DZN and their metabolites based on previously published models for the individual insecticides (Timchalk et al., 2002, 2007; Poet et al., 2004). This model has been designed to quantitatively integrate both tissue dosimetry and dynamic response (ChE inhibition) in blood and tissues. In addition, the metabolic interactions (CYP450) between CPF and DZN were evaluated *in vitro* to characterize the binary mixture enzymatic kinetic interactions for the OP mixture. Based on the *in vitro* metabolism results, the PBPK model code used to describe the CYP450 metabolism of CPF and DZN were appropriately modified to reflect the type of inhibition kinetics (i.e. competitive vs. non-competitive); while *B-est* metabolism was described as dose-additive, and no PON-1 interactions were assumed between CPF- and DZN-oxon with the enzyme. The binary model was then evaluated against previously published rodent dosimetry and ChE inhibition data for the mixture (Timchalk et al., 2005).

## 2. Materials and methods

### 2.1. In vitro metabolism

For the inhibition studies, samples were co-incubated with CPF and DZN. In general, the *in vitro* CYP450 metabolism studies, including sources of test material (CPF, DZN and their oxon metabolites) and metabolites standards (TCP and IMHP), animals, microsomal preparation, experimental conditions and analytical methods were as previously described by Poet et al. (2003).

### 2.2. In vitro data analysis

All hepatic microsomal incubations were conducted with $n = 3$–4 microsomal samples prepared from individual animals and means and standard deviations calculated. Metabolic rate constants were estimated using global non-linear regression analysis. The fit of equations describing competitive and non-competitive inhibition were evaluated using GraphPad Prism® (GraphPad Software, San Diego California USA, http://www.graphpad.com) which fits the family of curves with and without inhibitor using assigned concentrations of inhibitor (CPF or DZN) and determining best-fit $K_{m_{app}}$ and $V_{max_{app}}$ for all curves concurrently. The goodness of fit statistics available for GraphPad Prism® were used to determine which model (competitive or non-competitive) best described the data.

### 2.3. Model structure

A diagram of the PBPK/PD model structure is illustrated in Fig. 2A. The binary model was developed to describe the time-course of CPF, CPF-oxon, and TCP, as well as DZN, DZN-oxon and IMHP and the resulting inhibition of target esterases by the oxons in adult rats. This binary model was based on the previously published PBPK/PD models for CPF and DZN in both rats and humans, for a more detailed model description of the sources, assumptions and rational for parameter estimates, see Timchalk et al. (2002) and Poet et al. (2004). New research has made it possible to update a number of key model parameters including those associated with ChE inhibition, metabolism and tissue partition (Timchalk et al., 2002; Kousba et al., 2004, 2007; Lowe et al., 2006). Briefly, in the model CYP450 mediated activation of CPF or DZN to their respective oxon metabolites and their detoxification to TCP and IMHP, respectively, occurs only in the liver and is described as a Michaelis–Menten process. Equations used in physiologically based pharmacokinetic models to estimate extent and type of inhibition *in vivo* (Andersen et al., 1987) were applied to the model (see Fig. 2B). Inhibition of CYP450 metabolism ($K_i$) was described based on the results from the *in vitro* experiments, and were mathematically described as non-competitive (CPF or DZN → oxon, and CPF → TCP), or competitive (DZN → IMHP). PON-1 mediated metabolism of CPF-oxon and DZN-oxon occurs in the liver and blood and were likewise described as Michaelis–Menten processes. Interaction of CPF-oxon or DZN-oxon with the *B-est* AChE, BuChE, and CaE were modeled as second-order process. The *B-est* enzyme levels (μmol) were based on a balance between basal degradation and enzyme synthesis and the inhibition of *B-est* enzymes by CPF-oxon and DZN-oxon were modeled assuming a dose-additive response.

### 2.4. Model parameters

To develop the binary model, several types of data were required, including physiological constants, partitioning coefficients and biochemical constants describing the metabolism of CPF and DZN and *B-est* inhibition by their respective oxon metabolites. These data were obtained from the initially published individual models, from the literature, from experimentation, or by optimization of model output using computer simulation. The PBPK/PD model code for simultaneous solution of both algebraic and differential equations was developed in SIMUSOLV® (The Dow Chemical Do, Midland, MI), a computer program containing a numerical integration,

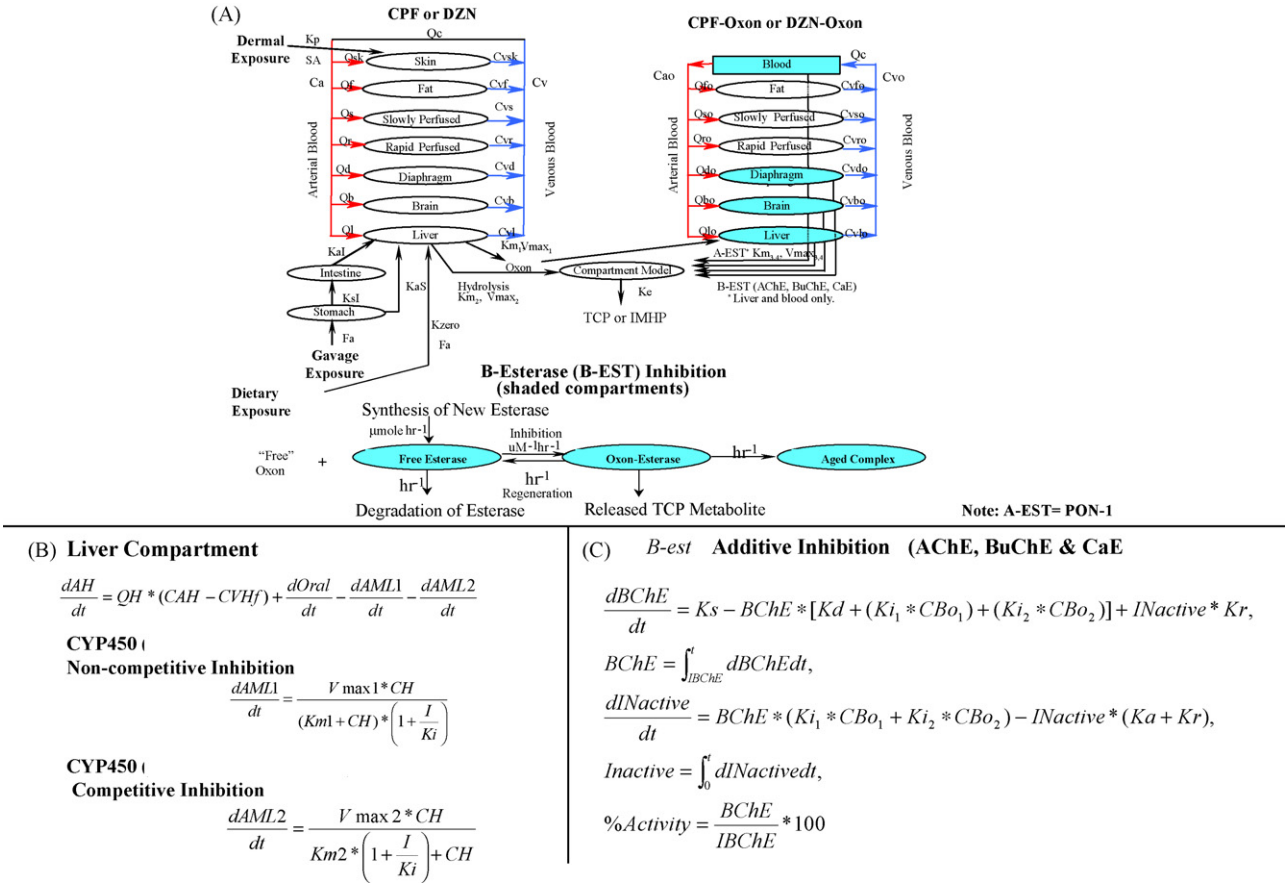


$$\frac{dAH}{dt} = QH*(CAH - CVHf) + \frac{dOral}{dt} - \frac{dAML1}{dt} - \frac{dAML2}{dt}$$

$$\frac{dAML1}{dt} = \frac{V\max 1*CH}{(Km1+CH)*\left(1+\frac{I}{Ki}\right)}$$

$$\frac{dAML2}{dt} = \frac{V\max 2*CH}{Km2*\left(1+\frac{I}{Ki}\right)+CH}$$

$$\frac{dBChE}{dt} = Ks - BChE*[Kd + (Ki_1*CBo_1) + (Ki_2*CBo_2)] + INactive*Kr,$$

$$BChE = \int_{IBChE}^{t} dBChEdt,$$

$$\frac{dINactive}{dt} = BChE*(Ki_1*CBo_1 + Ki_2*CBo_2) - INactive*(Ka+Kr),$$

$$Inactive = \int_{0}^{t} dINactivedt,$$

$$\%Activity = \frac{BChE}{IBChE}*100$$

Fig. 2. (**A**) Physiologically based pharmacokinetic and pharmacodynamic model used to describe the disposition of the parent insecticides chlorpyrifos (CPF) and diazinon (DZN), their oxon metabolites (CPF-oxon and DZN-oxon), trichloropyridinol (TCP), isopropyl-methyl-hydroxypyrimidine (IMHP) and *B-est* inhibition in rats following oral (gavage, dietary) and dermal exposures. The shaded tissues compartments indicate organs in which *B-est* (AChE, BuChE, and CaE) enzyme activity is described. Model parameter definitions: $Q_c$, cardiac output (L/h); $Q_i$, blood flow to "*i*" tissue (L/h), $C_a$, arterial blood concentration (μmol/L); $C_{ao}$, arterial blood concentration of oxon (μmol/L); $C_v$, pooled venous blood concentration (μmol/L); $C_{v_i}$, venous blood concentration draining "*i*" tissue (μmol/L); $C_{v_{i,o}}$, venous blood concentration of oxon draining "*i*" tissue (μmol/L); SA, surface area of skin exposed ($cm^2$); $K_P$, skin permeability coefficient (cm/h); $K_{zero}$, zero order (μmol/h) rate of absorption from diet; $F_a$, fractional absorption (%); *KaS* and *KaI*, first-order rate constants for absorption from compartments 1 and 2 ($h^{-1}$); *KsI* first-order rate constant for transfer from compartment 1 and 2 ($h^{-1}$); $K_e$, first-order rate constant for elimination of metabolite from compartment 3; $K_{m(1-4)}$, Michaelis constant for saturable processes (μmol/L); $V_{max(1-4)}$, maximum velocity for saturable process (μmol/h). (B) Differential equations used to describe CYP450 non-competitive (parent → oxon, parent → TCP) and competitive (parent → IMHP) inhibition in the liver compartment. Where CH is the concentration of CPF or DZN in the blood leaving the liver, $K_m$ is the Michaelis–Menten dissociation constant and $V_{max}$ is the Michaelis–Menten rate constant, $K_I$ is the dissociation constant for the enzyme–inhibitor complex and *I* is the inhibitor concentration. (C) Differential equations used to describe additive inhibition of CPF-oxon and DZN-oxon on brain AChE. Similar equations were used to describe additive BuChE and CaE inhibition in plasma, liver and diaphragm.

optimization and graphical routine, which is based on the Fortran-based software ACSL. To evaluate the fit of the model simulations to the experimental data the log likelihood function (LLF) was used as a criterion to assess the quality of the model fit to the data, with 100% indicating a perfect fit. Organ volumes, cardiac output, and tissue blood flows were obtained from the literature (Brown et al., 1997) and are summarized in Table 1.

### 2.5. Partition coefficients and biochemical constants

The partition coefficients and biochemical parameters used in the binary model are presented in Table 2. The partitioning coefficient for DZN and DZN-oxon were determined using an algorithm developed by Poulin and Krishnan (1995). This algorithm was originally used to determine CPF and CPF-oxon partitioning coefficients, but they have been updated based upon recently reported results (Lowe et al., 2006). The parameters ($K_m$ and $V_{max}$) for CYP450 metabolism of CPF or DZN to their oxon or TCP and IMHP metabolites were based on previous *in vitro* determinations (Poet et al., 2003). In some cases the $K_m$ values were optimized to fit the experimental data. The metabolic parameters ($K_m$ and $V_{max}$) for the PON-1 liver and blood esterase metabolism of CPF-oxon were based on metabolism studies reported by Mortensen et al. (1996). Parameter estimates for both CYP450 and PON-1 metabolism of DZN and DZN-oxon were determined *in vitro* using hepatic microsomes in a previous study (Poet et al., 2003), as described (Poet et al., 2004).

### 2.6. B-esterase (B-est) inhibition

The model structure for the inhibition of *B-est* (AChE, BuChE and CaE) in plasma, RBC, brain, diaphragm and liver is

Table 1
General physiological parameters used in the PBPK/PD model for CPF and DZN

| Parameter | CPF and DZN |
|---|---|
| Body weight (kg) | 0.274–0.303 |
| Tissue volume (% of body weight) | |
| Blood | 6.0 |
| Brain | 1.2 |
| Diaphragm | 0.03 |
| Liver | 4.0 |
| Rapid perfused | 4.0 |
| Slowly perfused | 78 |
| Fat | 7.0 |
| Cardiac output (L/kg/h) | 15 |
| Percentage of cardiac output (%) | |
| Liver | 25 |
| Brain | 7.0[a] |
| Diaphragm | 0.6 |
| Rapid perfused | 44 |
| Slowly perfused | 14 |
| Fat | 9.0 |

[a] Optimized parameter.

based on the previous published model structure for CPF and DZN (Timchalk et al., 2002; Poet et al., 2004), and the model parameter estimates are presented in Table 3. The *B-est* enzyme levels (μmol) in blood (plasma and RBC), brain, liver and diaphragm were calculated based on the enzyme turnover rates and enzyme activities reported by Maxwell et al. (1987). The inhibition of *B-est* enzymes by CPF-oxon and DZN-oxon were modeled assuming a dose-additive response based on the equation illustrated in Fig. 2C. The enzyme degradation ($K_d$) rates for AChE, BuChE and CaE were initially based on the first-order loss of rat brain AChE as described by Gearhart et al. (1990). In general, BuChE activity is similar to AChE and as a first approximation the synthesis and loss rates for BuChE were set the same as for AChE. Whereas, for CaE, reasonable parameter estimates for synthesis and loss rates were not available so the rates were optimized with the PD model to fit CaE inhibition data from Chanda et al. (1997) (Timchalk et al., 2002).

For the additive inhibition model (see Fig. 2C), *dBChEdt* is the rate of change (μmol/h) of brain AChE enzyme; $K_s$ is the zero-order enzyme synthesis rate (μmol/h); *BChE* is the amount (μmol) of available enzyme; $K_d$, $K_r$ and $K_a$ are the first-order rates ($h^{-1}$) for enzyme degradation, regeneration and aging, respectively; $K_{i_1}$ and $K_{i_2}$ $(\mu M\ h)^{-1}$ are the bimolecular inhibition rates constants; while $CBo_1$ and $CBo_2$ are the concentration (μmol/L) for CPF-oxon and DZN-oxon, respectively. "*INactive*" is the amount (μmol) of AChE that is inactive due to phosphorylation of the enzyme, and *IBChE* is the initial brain AChE concentration. The percent (%) of enzyme activity is expressed as the ratio between the amount of available enzyme (*BChE*) and the initial levels (*IBChE*). Similar equations were used to describe BuChE and CaE inhibition in tissues and blood compartments.

## 3. Results

### 3.1. In vitro CYP-mediated metabolism

Both CPF and DZN were metabolized *in vitro* to their corresponding oxons and pyridinol/pyrimidinol metabolites in hepatic microsomes prepared from naïve rats. Current computer capabilities allow for simple rate constant calculations using the Michaelis–Menten equation without using a linear transformation and result in improved data estimation. GraphPad Prism® was used to individually determine metabolic parameters for DZN with and without fixed concentrations of CPF and for CPF with and without fixed DZN concentrations to determine $V_{max_{app}}$, $K_{m_{app}}$, and $K_{i_{app}}$. The *in vitro* competitive metabolism results for CPF and DZN are presented in Fig. 3 and Table 4 along with the corresponding GraphPad Prism® fit of the data. The comparison of *in vitro* metabolism for CPF and DZN suggests that CPF is more substantially metabolized to its oxon metabolite than is DZN; whereas, DZN CYP450 metabolism appears to favor the IMHP pathway. These *in vitro* findings are consistent with the observed *in vivo* relative potency (CPF > DZN) of these OP insecticides. For both OP insecticides they each inhibited the other's *in vitro* metabolism in a concentration-dependent manner. The metabolism of DZN to DZN-oxon, and CPF to CPF-oxon and TCP were best-fit using a non-competitive inhibition equation, which results in an increase in the apparent $K_m$ ($K_{m_{app}}$) with increasing concentration of the inhibitor; this is further illustrated in the double-reciprocal plots for both oxons and TCP (see Fig. 3A–C, insets). In the case of DZN, metabolism to form IMHP is best-fit using a competitive inhibition equation (Fig. 3D). The average $K_{i_{app}}$ was subsequently utilized as the CYP450 inhibition constant in the binary PBPK/PD model, using the equation for either competitive or non-competitive inhibition.

### 3.2. Pharmacokinetics

The previously determined time-course of CPF and DZN and their metabolites IMHP and TCP in blood following oral administration of either individual chemicals or as a binary mixture at doses of 15 and 60 mg/kg (Timchalk et al., 2005) are shown in Figs. 4 and 5, along with the PBPK/PD model fits (solid lines) to these experimental data. The percentage of variation explained based on the maximum log likelihood function for the model simulations for each of the experimental data sets is presented in Table 5. At 15 mg/kg, model simulations of peak blood concentrations of DZN and CPF were consistent with the experimental data, being attained by ~3 h post-dosing for both pesticides. The PBPK/PD model was consistent with the overall CPF blood time-course (Fig. 4A), but over-predicted the DZN results (Fig. 4C). For TCP and IMHP metabolites, peak blood levels following a single chemical exposure at 15 mg/kg were achieved by ~6 and 3 h post-dosing, respectively, and the simulated $C_{max}$ for TCP and IMHP were consistent with the experimental results and very comparable (6.5 μmol/L vs. 7.4 μmol/L, respectively). The

Table 2
CPF and DZN specific parameters used in the PBPK/PD model

| Parameter | CPF | CPF-oxon | DZN | DZN-oxon | Estimation method |
|---|---|---|---|---|---|
| Partition coefficients | | | | | |
| Brain/blood | 15.1[a] | 8.3[a] | 28[b] | 10.9[b] | Lowe et al. (2006)[a] |
| Diaphragm/blood | 3.6[a] | 2.3[a] | 5.2[b] | 2.3[b] | Calculated[b] |
| Fat/blood | 228[a] | 119[a] | 361[b] | 123[b] | |
| Liver/blood | 11.7[a] | 6.5[a] | 18.1[b] | 7.0[b] | |
| Rapid perfused/blood | 3.6[a] | 2.3[a] | 18.1[b] | 3.5[b] | |
| Slow perfused/blood | 3.6[a] | 2.3[a] | 5.2[b] | 2.3[b] | |
| Metabolic constants | | | | | |
| CYP450 CPF to CPF-oxon/DZN to DZN-oxon (liver) | | | | | |
| $K_m$ (μmol/L) | 0.93[d] | – | 5[c] | – | Optimized[c] |
| $V_{maxC}$ (μmol/h/kg) | 14.3[d] | – | 14[d] | – | Poet et al. (2003)[d] |
| Inhibition: DZN on CPF to CPF-oxon and CPF on DZN to DZN-oxon | | | | | |
| $K_i$ (μmol/L) | 174[e] | – | 204[e] | – | Measured[e] |
| CYP450 CPF to TCP/DZN to IMHP (liver) | | | | | |
| $K_m$ (μmol/L) | 5.1[d] | – | 200[d] | – | Poet et al. (2003)[d] |
| $V_{maxC}$ (μmol/h/kg) | 60.9[d] | – | 180[d] | – | |
| Inhibition: DZN on CPF to TCP and CPF on DZN to IMHP | | | | | |
| $K_i$ (μmol/L) | 84.9[e] | – | 63.6[e] | – | Measured[e] |
| PON-1 CPF-oxon to TCP/DZN-oxon to IMHP (liver) | | | | | |
| $K_m$ (μmol/L) | – | 850[c] | – | 270[j] | Optimized[c] |
| $V_{maxC}$ (μmol/h/kg) | – | 38,002[f] | – | 63,000[j] | Mortensen et al. (1996)[f] |
| PON-1 CPF-oxon to TCP/DZN-oxon to IMHP (blood) | | | | | |
| $K_m$ (μmol/L) | – | 450[c] | – | 270[j] | Optimized[c] |
| $V_{maxC}$ (μmol/h/kg) | – | 40,377[f] | – | 63,000[j] | Mortensen et al. (1996)[f] |
| Oral absorption parameters | | | | | |
| *KaS* (stomach; $h^{-1}$) | 0.01[g] | – | 0.068[j]<br>2.1E−5[c,k] | – | Timchalk et al. (2002)[g]<br>Timchalk et al. (2007)[h] |
| *KaI* (intestine; $h^{-1}$) | 0.5[g] | – | 0.058[j]<br>0.321[c,k] | – | Lowe et al. (2006)[i]<br>Poet et al. (2004)[j] |
| *KsI* (transfer stomach–intestine; $h^{-1}$) | 0.5[g] | – | 0.21[j]<br>0.321[c,k] | – | |
| $F_a$ (fractional abs; %) | 100 | – | 100 | – | |
| Protein binding (%) | 95[g,h] | 95[g,h] | 89[j] | 89[j] | |

| | TCP | IMHP | |
|---|---|---|---|
| TCP and IMHP model parameters | | | |
| $V_d$ (L) | 1.11[c] | 0.185[c] | Optimized[c]<br>Poet et al. (2004)[j] |
| $K_e$ ($h^{-1}$) | 0.126[c] | 0.138[c] | |
| $K_1$ (first-order rate loss) | – | 0.55[j] | |

The model parameters were estimated independently and held fixed, calculated or fitted as previously described (Timchalk et al., 2002; Poet et al., 2004). The superscript designates sources of the parameter a–j (estimation method).
[k] Parameter estimate for DZN:CPF (60/60, mg/kg) group only.

PBPK/PD model simulations of the binary-exposure (15 + 15 mg/kg) resulted in no differences in the predicted pharmacokinetics of either the parent OPs or their respective metabolites, which was consistent with the experimental results.

A similar pharmacokinetic analysis of CPF, DZN, and their metabolites following a high dose single- (60 mg/kg) or binary-exposure (60 + 60 mg/kg) to CPF and DZN in the rat was also conducted (Timchalk et al., 2005). The experimental data and model simulations are presented in Fig. 5. Administering a binary dose of CPF + DZN at 60 + 60 mg/kg did result in observable changes in the DZN pharmacokinetics (relative to DZN-only 60 mg/kg), where peak blood concentrations were slightly delayed (6 h vs. 3 h post-dosing) and increased to 2.84 ± 0.39 from 0.59 ± 0.19 μmol/L (see Fig. 5C). For CPF, a high binary dose of CPF + DZN (60 + 60 mg/kg) likewise shifted the time to peak blood concentration from 3 to 6 h post-dosing, but resulted in only a slight increase in CPF peak blood concentrations (5.03 ± 1.21 μmol/L vs. 3.24 ± 2.25 μmol/L). These binary-exposures appeared to have minimal impact on the TCP and IMHP pharmacokinetics (Fig. 5B and D). For CPF and its metabolite TCP, PBPK model simulations slightly

Table 3
Parameters used in the pharmacodynamic model for CPF-oxon and DZN-oxon inhibition of AChE, BuChE and CaE

| Enzymes | Turnover rate[a] (enzyme hydrolysis, $h^{-1}$) |
|---|---|
| AChE | 1.17 E+7 |
| BuChE | 3.66 E+6 |
| CaE | 1.09 E+5 |

| Tissue | Enzyme activity (μmol/kg/h)[a] | | |
|---|---|---|---|
| | AChE | BuChE | CaE |
| Brain | 4.4 E+5 | 4.68 E+4 | 6.0 E+4 |
| Diaphragm | 7.74 E+4 | 2.64 E+4 | 3.18 E+5 |
| Liver | 1.02 E+4 | 3.00 E+4 | 1.94 E+6 |
| Plasma | 1.32 E+5 | 1.56 E+4 | 4.56 E+5 |

| | Esterase parameters[b] | | | | |
|---|---|---|---|---|---|
| | Enzyme degradation rates ($h^{-1}$) | Enzyme reactivation rates ($h^{-1}$) | Enzyme aging rates ($h^{-1}$) | Bimolecular inhibition $K_i$ ($\mu M\ h)^{-1}$ CPF-oxon | Bimolecular inhibition $K_i$ ($\mu M\ h)^{-1}$ DZN-oxon |
| AChE | | | | | |
| Brain, diaphragm, liver[c], plasma[c] | 0.01 | 0.014 | 0.0113 | 243 | 525 |
| RBC | 0.008 | 0.014[c] | 0.0113 | 243[c] | 525 |
| BuChE | | | | | |
| Brain, diaphragm, liver[c], plasma[c] | 0.01 | 0.014 | 0.0113 | 2000 | 1700 |
| CaE | | | | | |
| Brain | 7.54 E−4 | 0.014 | 0.0113 | 20 | 0.5 |
| Diaphragm, liver | 0.001 | 0.014 | 0.0113 | 20 | 0.5 |
| Plasma | 0.0033 | 0.0143 | 0.0113 | 20 | 0.5 |

The model parameters were estimated independently and held fixed, calculated or fitted as previously described (Timchalk et al., 2002).
[a] Maxwell et al. (1987).
[b] Timchalk et al. (2002) and Poet et al. (2004).
[c] Parameter estimates have been updated from published value in Timchalk et al. (2002).

Table 4
Metabolic rate constants for CPF or DZN Co-incubations

| | $K_{m_{app}}$ (μmol/L) | $V_{max_{app}}$ (μmol/h/kg) | $K_{i_{app}}$ (μmol/L) | Model |
|---|---|---|---|---|
| DZN inhibition of CPF | | | | |
| TCP | 25.11 ± 3.35 | 1.04 ± 0.0507 | 84.9 ± 9.01 | Non-competitive |
| CPF-oxon | 83.3 ± 14.2 | 0.557 ± 0.0483 | 174 ± 26.7 | Non-competitive |
| CPF inhibition of DZN | | | | |
| IMHP | 263 ± 23.2 | 4.00 ± 0.154 | 63.6 ± 4.39 | Competitive |
| DZN-oxon | 136 ± 24.4 | 0.207 ± 0.0137 | 204 ± 27.2 | Non-competitive |

underpredicted peak blood CPF, while more reasonably simulating the TCP time-course data. Attempts were made to improve the fit to the CPF binary-exposure data sets, by optimizing the absorption parameters (*KaS*, *KaI* and *KsI*), but this did not result in any appreciable improvement (data not shown). Whereas, for DZN and IMHP optimizing the absorption parameters substantially improve the DZN $C_{max}$ fit for the binary dose by both increasing the model predicted $C_{max}$ of DZN from 1.03 to 3.02 μmol/L while shifting the time to peak concentration from ~2 to 4 h post-dosing. The slower absorption rate for DZN also positively impacted the fit to the IMHP blood time-course, at least through 12 h post-dosing (see Fig. 5D).

Table 5
Percentage (%) variation explained based on maximized log likelihood function analysis for the binary PBPK/PD models for chlorpyrifos (CPF) and diazinon (DZN) co-exposures

| Fit to experimental data | CPF | DZN | [a]DZN (60 + 60 mg/kg) |
|---|---|---|---|
| Overall | 88 | 77 | 79 |
| Blood CPF | 67 | – | – |
| Blood TCP | 93 | – | – |
| Blood DZN | – | 35 | 60 |
| Blood IMHP | – | 79 | 91 |
| Plasma ChE | 91 | 76 | 89 |
| RBC AChE | 65 | 72 | 72 |
| Brain AChE | 85 | 88 | 81 |

[a] Optimized absorption parameters *KaS*, *KaI* and *KsI*.

### 3.3. Pharmacodynamics

The PBPK/PD model was also used to simulate the corresponding ChE inhibition dynamics in plasma, RBC and brain following single- or binary-exposures to CPF and DZN (Timchalk et al., 2005) and the fit to these experimental data are

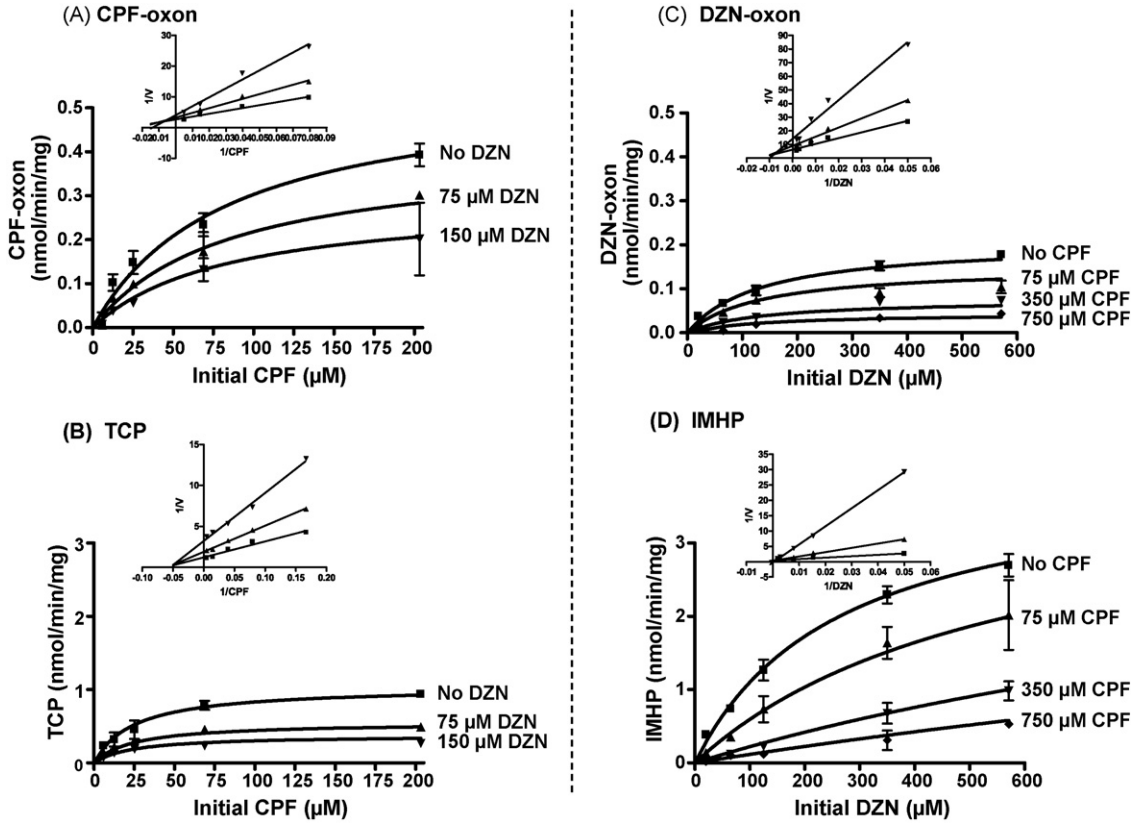


Fig. 3. *In vitro* CYP450 mediated metabolism of chlorpyrifos (CPF) to (A) CPF-oxon and (B) trichloropyridinol and the metabolism of diazinon (DZN) to (C) DZN-oxon and (D) isopropyl-methyl-hydroxypyrimidine (IMHP) in microsomes prepared from naïve adult Sprague–Dawley rats. The competitive metabolism studies were conducted by co-incubation with increasing concentrations of the competing parent OP. The fit to the experimental data were obtained using GraphPad Prism®, and the graphical inserts are the corresponding Lineweaver–Burk reciprocal plots.

presented in Figs. 6–8. As previously reported, the degree of experimentally determined ChE inhibition was generally dose-dependent, the extent of inhibition followed plasma >RBC ≥ brain, and the relative potency was CPF + DZN ≥ CPF ≫ DZN (Timchalk et al., 2005). In general, the PBPK/PD model response across tissues, dose, time, and for the single- and binary-exposures was consistent with the experimental findings.

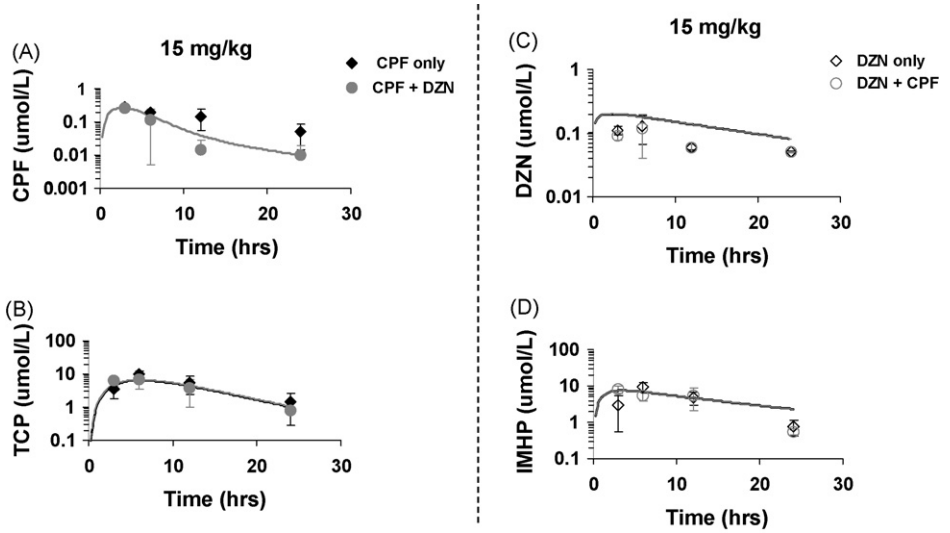


Fig. 4. The concentration of (A) chlorpyrifos (CPF), (B) trichloropyridinol (TCP), (C) diazinon (DZN) and (D) isopropyl-methyl-hydroxypyrimidine (IMHP) in the blood of Sprague–Dawley rats following an oral gavage dose of 15 mg/kg CPF (filled black diamond) or DZN (open black diamond) as single chemicals or as a binary mixture (15/15, mg/kg) of DZN/CPF (filled and open gray circles). The data are expressed as concentration (μmol/L) over time (h) and represent the mean ± S.D. of 4 animals per time-point. The lines represent the PBPK/PD model simulations.

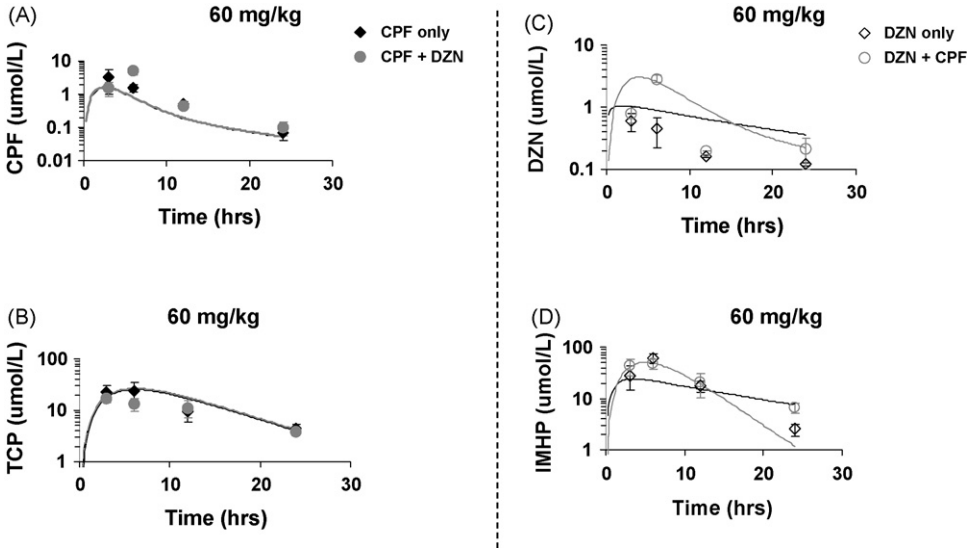


Fig. 5. The concentration of (A) chlorpyrifos (CPF), (B) trichloropyridinol (TCP), (C) diazinon (DZN) and (D) isopropyl-methyl-hydroxypyrimidine (IMHP) in the blood of Sprague–Dawley rats following an oral gavage dose of 60 mg/kg CPF (filled black diamond) or DZN (open black diamond) as single chemicals or as a binary mixture (60/60, mg/kg) of CPF/DZN (filled and open gray circles). The data are expressed as concentration (μmol/L) over time (h) and represent the mean ± S.D. of 4 animals per time-point.

The time-course of plasma ChE inhibition in rats following oral exposure to single- or binary-doses of CPF and DZN is presented in Fig. 6. Consistent with the experimental finding, model simulations suggest that CPF has a substantially greater inhibitory impact on plasma ChE activity than DZN at all dose levels. The model also tends to under-predict the DZN-only response (Fig. 6D–F), but more accurately simulated the CPF-only and CPF + DZN mixture inhibition. For the CPF-only and CPF + DZN binary mixture the plasma ChE response were very comparable with the simulation of maximum inhibition ranging tightly from 18 to 16, 6.2 to 5.2 and 2.2 to 1.9% of control activity for both the single- and binary-exposures to CPF and CPF + DZN (15, 30 and 60 mg/kg, respectively). In contrast, the model consistently under-predicts the DZN plasma ChE

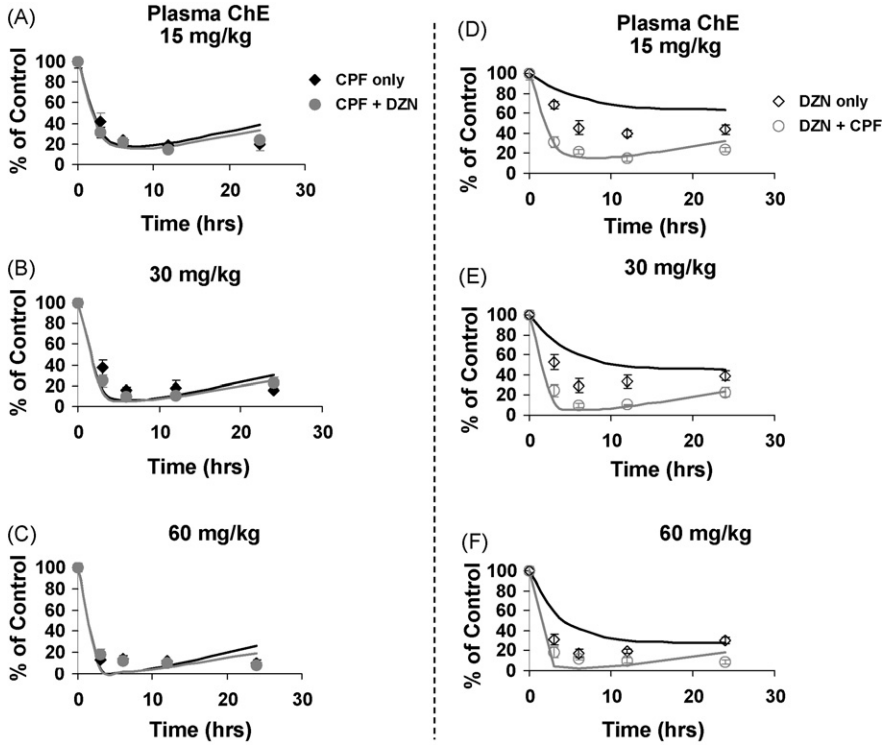


Fig. 6. Plasma cholinesterase (ChE) activity in Sprague–Dawley rats following 15, 30, or 60 mg/kg oral gavage doses of chlorpyrifos (CPF) (solid black diamond), diazinon (DZN) (open black diamond) and their binary mixtures (solid or open gray circle). The data are expressed as % of total ChE activity as a function of time (h) and represents the mean ± S.D. for 4 animals per time-point. The lines represent the PBPK/PD model simulations.

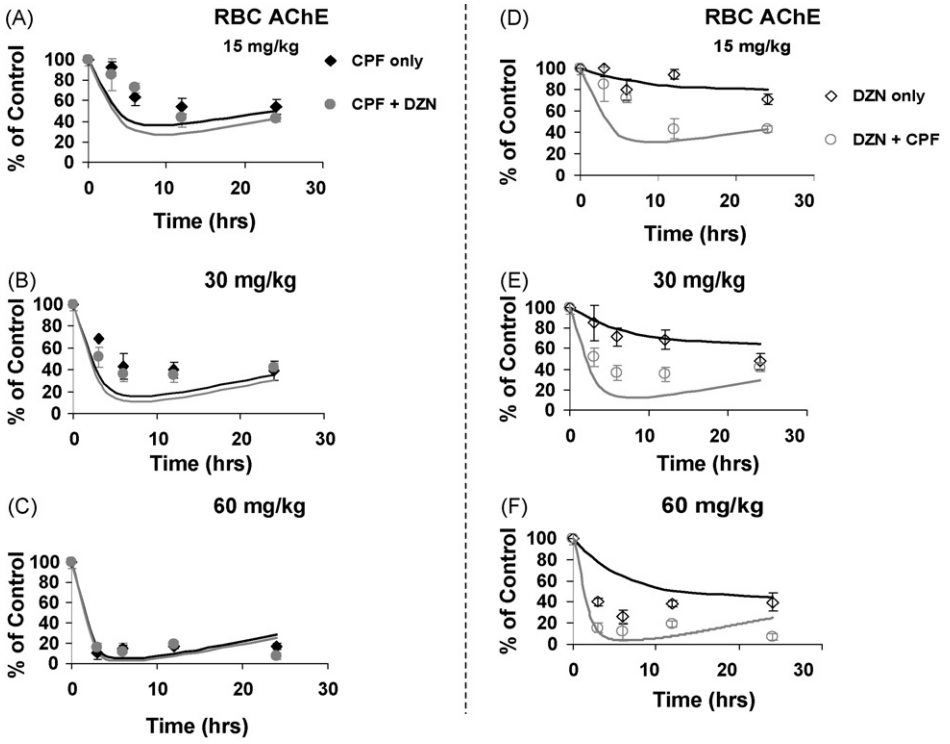


Fig. 7. Red blood cell (RBC) acetylcholinesterase (AChE) activity in Sprague–Dawley rats following 15, 30, or 60 mg/kg oral gavage doses of chlorpyrifos (CPF) (solid black diamond), diazinon (DZN) (open black diamond) and their binary mixtures (solid or open gray circle). The data are expressed as % of total ChE activity as a function of time (h) and represents the mean ± S.D. for 4 animals per time-point. The lines represent the PBPK/PD model simulations.

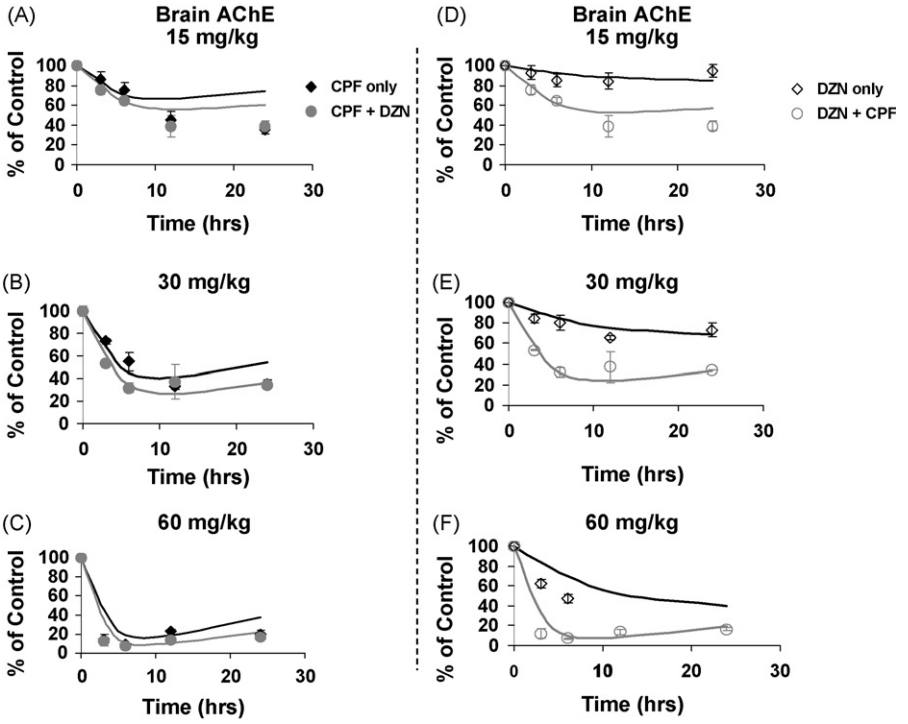


Fig. 8. Brain acetylcholinesterase (AChE) activity in Sprague–Dawley rats following 15, 30, or 60 mg/kg oral gavage doses of chlorpyrifos (CPF) (solid black diamond), diazinon (DZN) (open black diamond) and their binary mixtures (solid or open gray circle). The data are expressed as % of total ChE activity as a function of time (h) and represents the mean ± S.D. for 4 animals per time-point. The lines represent the PBPK/PD model simulations.

inhibition; however, both the experimental results and model simulations suggest that plasma ChE inhibition for a single-exposure to DZN at doses of 15 or 30 mg/kg resulted in substantially less ChE inhibition. Only at the 60 mg/kg dose (Fig. 6F) is near maximum inhibition achieved for both DZN and CPF + DZN.

The RBC AChE inhibition following CPF and DZN single- or binary-exposures is presented in Fig. 7, and the overall dose-, mixture- and time-dependent response is consistent with the experimental data and comparable to the response seen with plasma ChE. Again, the experimental data and model simulations suggest that CPF has a substantially greater impact on the extent of RBC AChE inhibition relative to DZN. For the CPF and CPF + DZN exposures at 15 and 30 mg/kg, experimentally determined peak RBC AChE inhibition was observed at ~12 h post-dosing, whereas the PBPK/PD model simulated peak inhibition at ~6 h post-dosing and slightly over-predicted the maximum inhibition in these groups (Fig. 7A and B). Whereas, at these same doses (15 and 30 mg/kg) the model simulation of the RBC AChE and experimental data following the DZN-only dose were consistent, suggesting that maximum inhibition was achieved by 24 h post-dosing. For the DZN-only 15 and 30 mg/kg doses experimentally determined peak RBC AChE inhibition were 71 ± 5 and 48 ± 8% of control activity with corresponding model simulations of 79 and 64% of control activity, respectively (see Fig. 7D and E). For the 60 mg/kg single- and binary-exposure groups the PBPK/PD model under predicts the extent of RBC AChE inhibition following a DZN-only dose, but does describe the maximum inhibition following the CPF-only and CPF + DZN binary-exposures.

The dose-, time- and mixture-dependent inhibition of brain AChE following single- or binary-exposures to CPF and DZN are presented in Fig. 8. The general response and model simulations are also consistent with the pharmacodynamics observed for plasma ChE and RBC AChE inhibition. Initial simulations of the experimental data had 3% of the cardiac output to the brain compartment, which consistently under-predicted the AChE inhibition kinetics (data not shown). Therefore, we arbitrarily set flow to the brain at 7% which resulted in a better fit to the experimental data. As previously reported in the brain there is a potential shift towards shorter times to achieve maximum inhibition with increasing doses of CPF and DZN (Timchalk et al., 2005), which is reasonably simulated by the PBPK/PD model. Consistent with the experimental finding, model simulations suggest that CPF has a substantially greater inhibitory impact on brain AChE activity than DZN at all dose levels.

The general modeling strategy was to simultaneously simulate/fit all the data from a given experiment. For example, in evaluating the CPF model, the data presented in Figs. 4 and 5(A and B) and 6–8(A–C) were simultaneously fit, such that the model could simulate dose-dependent and mixture interactions

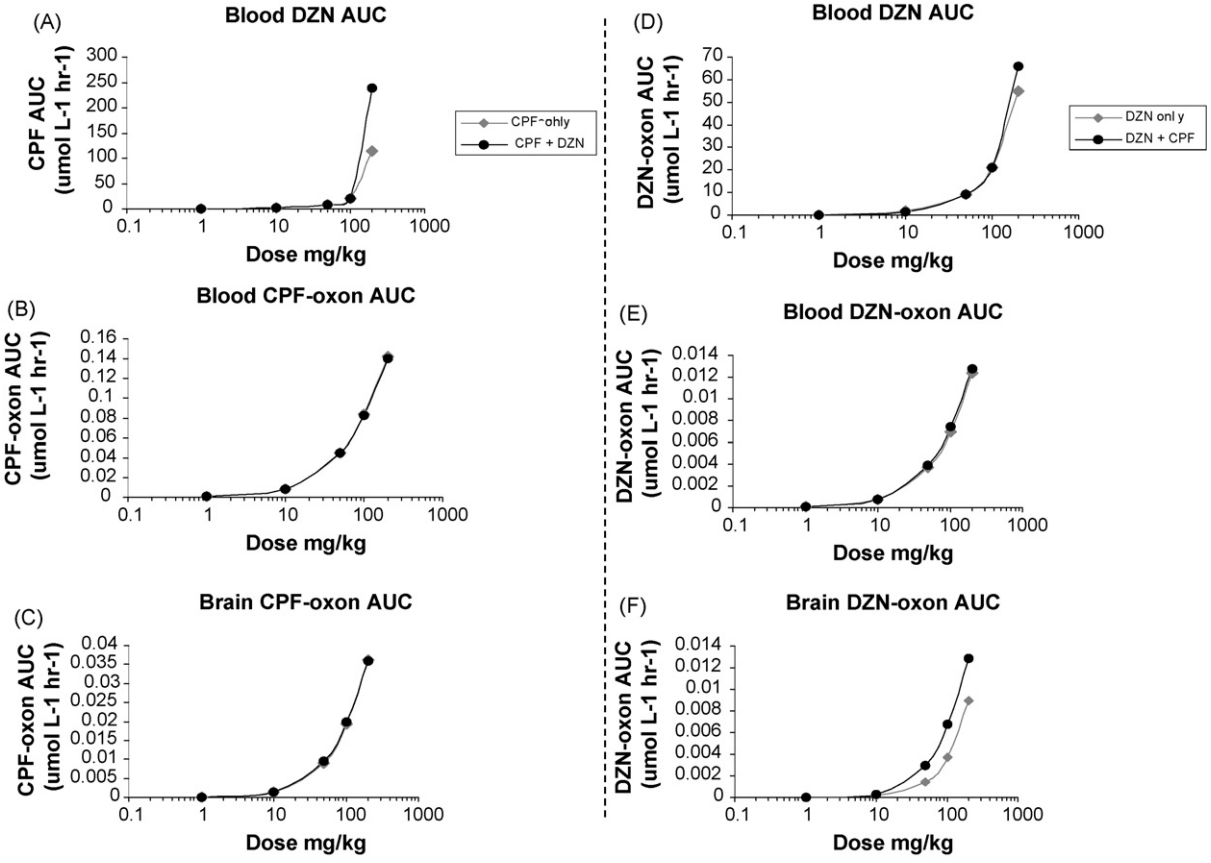


Fig. 9. Model simulation of chlorpyrifos (CPF), diazinon (DZN), CPF-oxon and DZN-oxon area-under-the-concentration (AUC) curve for single- and binary-exposures to CPF and DZN over a broad range of doses (1–200 mg/kg). The solid gray diamonds represent CPF and DZN as single doses, while the solid black circles represent the binary mixture.

on both pharmacokinetic and pharmacodynamic endpoints. A similar approach was used to evaluate DZN. To provide some perspective on the goodness of the model fit, the percentage of variation explained based on a maximum log likelihood function for simulations conducted with each of the experimental data sets is presented in Table 5. In general, the PBPK/PD model did a slightly better job of providing an overall fit for CPF than DZN (88% vs. 70–77%), however for both insecticides the model fits to the CPF and DZN blood time-courses were the poorest. In the case of the DZN + CPF mixture (60 + 60 mg/kg) modifying the absorption rates did result is some improvement in the overall fit (60% vs. 35%). In contrast, reasonably good fits were obtained for the blood TCP and IMHP (93% vs. 79–91%); again in the case of the high dose DZN + CPF mixture, optimizing absorption substantially improved the % variation explained. In general, the model provided a reasonable simulation of the pharmacodynamics. For the CPF experiments the % variation explained across all doses and treatments ranged from 91 to 85% with the plasma ChE > brain AChE > RBC AChE. Whereas, for the DZN group the % variation explained ranged from 89 to 72% with brain AChE ≥ plasma ChE > RBC AChE.

The PBPK/PD model was utilized to further evaluate theoretical mixture interactions over a very broad range of CPF and DZN doses. In these simulations (see Fig. 9) single acute doses ranging from 1 to 200 mg/kg were evaluated, recognizing that the high end of the dose range (50–200 mg/kg) would result in substantial adverse acute toxicity, including lethality. The rationale for simulating these very high acute doses was to try and establish at what dosage the model would predict a deviation between the single- and binary-exposures. Only a binary-exposure (CPF + DZN) at dose levels greater than ~200 + 200 mg/kg resulted in a theoretical increase (~2×) in the CPF AUC relative to CPF-only (see Fig. 9A). However, the binary-exposure had no impact on the CPF-oxon AUC in either the blood or brain compartments at the highest doses simulated (Fig. 9B and C). In evaluating the impact of co-exposure on DZN dosimetry, binary-exposures greater than 10 + 10 mg/kg, did result in a slight increase in the DZN-oxon brain AUC (1–3×). These simulations are very consistent with the experimental findings and suggest that binary interactions between CPF and DZN at environmentally relevant exposures levels will most likely be negligible and that CPF has a greater impact than DZN as a binary mixture.

## 4. Discussion

Organophosphorus insecticides have routinely been used to control pests in virtually all crop and commercial applications (Cal EPA, 1998); therefore, it is entirely feasible to anticipate exposure to insecticide mixtures. This conclusion is supported by a number of biomonitoring studies which have measured the presence of several OP metabolites in urine, and reported the inhibition of plasma ChE in these same workers (Lavy et al., 1993; Hayes et al., 1980). The potential for OP insecticides to produce a toxic response is dependent upon the balance between the amount of delivered dose to the target site and the rates of bioactivation and/or detoxification (Calabrese, 1991). In this regard, CPF and DZN are structurally similar phosphorothionate insecticides that share common biotransformation pathways (see Fig. 1), a common mode of toxicological action (i.e. ChE inhibition), yet quantitatively differ with regard to the extent of metabolism (Poet et al., 2003) and the degree of ChE inhibition (Timchalk et al., 2002, 2005; Poet et al., 2004). Based upon this common mode of action, there is a need to better understand the potential for cumulative toxicity (Mileson et al., 1998), particularly for structurally related OP insecticides. It has been suggested that PBPK and PBPK/PD modeling along with focused *in vitro* and *in vivo* experimentation can be exploited to quantitatively evaluate binary and more complex mixture interactions, which can then be utilized to evaluate risk from these chemical mixture exposures (Yang et al., 1995; el-Masri et al., 1997; Krishnan et al., 2002). Hence, the objective of the current study was to develop a binary PBPK/PD model to evaluate the potential pharmacokinetic and pharmacodynamic interactions for a mixture of CPF and DZN in the rat.

In developing the binary PBPK/PD OP model, the similar metabolic and mode of action (i.e. ChE inhibition) properties for CPF and DZN suggested that these OP insecticides have the potential to interact at both a pharmacokinetic and pharmacodynamic level. To experimentally evaluate this, *in vivo* interaction studies for a binary mixture of CPF and DZN were conducted in rats (Timchalk et al., 2005). These data suggested that observed changes in $C_{max}$ and AUC at high binary doses of CPF + DZN might be due to competition between CPF and DZN for CYP450 (microsomal) metabolism. Secondly, a comparison of the ChE response at lower doses where there are no apparent pharmacokinetic interactions for a binary mixture suggested that the overall ChE response was dose-additive. This conclusion was consistent with Richardson et al. (2001) who suggested that *in vitro* interactions of CPF-oxon and azinophosmethyl-oxon with brain AChE were best characterized using a dose-additive model since the extent of AChE inhibition is dependent upon the relative potency of each oxon for the enzyme. Hence, in developing the binary PBPK/PD model, *in vitro* competitive metabolism studies were conducted to characterize the metabolic interactions, and a dose-additive model for ChE inhibition was assumed.

A number of studies have compared the *in vitro* CYP450 metabolism of both CPF and DZN in human and rodent microsomal and cellular systems expressing human CYPs (Fabrizi et al., 1999; Sams et al., 2000; Tang et al., 2001; Buratti et al., 2002, 2003). These studies indicate that the CYP450 metabolism of CPF and DZN do share a number of common CYP450 enzymes. In the current study, the major metabolites formed from CYP-mediated *in vitro* hepatic metabolism from both CPF and DZN are the inactive TCP and IMHP metabolites with the active oxons representing the minor metabolites, which is consistent with previous findings (Ma and Chambers, 1994; Fabrizi et al., 1999; Tang et al., 2001; Poet et al., 2003). However, the current study also evaluated the metabolic interactions between DZN and CPF and based upon the current analysis the formation of CPF- and DZN-oxon as well as TCP

and IMHP were metabolically inhibited under co-incubation conditions. Analysis of the data suggested that CPF competitively inhibited the metabolism of DZN to IMHP, whereas, all other metabolic interactions were best described as non-competitive inhibition (see Fig. 3). A time-dependence on inhibition of all but IMHP metabolism suggests that chlorpyrifos and diazinon are suicide substrates (data not shown), consistent with observations for other OPs (Halpert et al., 1980; Hodgson and Rose, 2006; Joo et al., 2007). Although inhibition was clearly demonstrated, the calculated average $K_{i_{app}}$ for inhibition of CPF and DZN metabolism was fairly high suggesting that *in vivo* kinetic interactions would only be observed at very high binary doses, consistent with previously reported results (Timchalk et al., 2005).

The binary PBPK/PD model code was constructed using the model framework that was previously developed for CPF then adapted for DZN by our research group (Timchalk et al., 2002; Poet et al., 2004). As previously discussed, the integrated binary model was primarily modified to describe hepatic CYP450 non-competitive and competitive Michaelis–Menten metabolism based on the *in vitro* metabolism studies. Secondly, the binary model modified the pharmacodynamics to be dose-additive for CPF- and DZN-oxon interactions with tissue ChE. A number of other parameters have been updated or refined as new insights or experimental data have become available. A particular limitation for the development and validation of the binary model is the lack of robust *in vitro* and *in vivo* mixture studies for CPF and DZN. Hence, only the limited *in vivo* rodent studies previously conducted in our laboratory (Timchalk et al., 2005), and *in vitro* studies reported in this manuscript were available for model development. It is anticipated that as additional mixture studies in animal models or relevant human biomonitoring data become available that further refinement and validation of the binary model will be possible.

In reporting the *in vivo* pharmacokinetic interactions for CPF and DZN it was obvious that co-exposure to a binary dose of 15 + 15 mg/kg did not appreciably impact the pharmacokinetics or metabolism of either pesticide; whereas, a binary 60 + 60 mg/kg dose did result in a slight disproportionate increase in $C_{max}$ and AUC for both CPF and DZN (Timchalk et al., 2005), with the changes greatest for DZN. It was suggested that the increase in $C_{max}$ at the higher dose could be related to the saturation of the initial CYP450 metabolism and/or shifts in the extent of oral absorption. However, initial PBPK/PD model simulation of the time-courses of CPF, TCP, DZN and IMHP following single- or binary-exposures suggested that pharmacokinetics of the parent insecticides or their metabolites were linear and not impacted by co-exposures, yet the kinetics particularly for the higher dose (60 + 60 mg/kg) DZN binary-exposure (Fig. 5C) did suggest a substantial spike increase in the $C_{max}$ at 6 h post-dosing. Hence, in an attempt to more reasonably fit the experimental data, the gut absorption parameters (*KaS*, *KaI* and *KsI*) for DZN were optimized, which improved the model fit to the peak blood concentrations for both DZN and IMHP. Attempts were also made to improve the fit for the CPF blood time-course, by modifying absorption rates; however, this did not result in any substantial improvements. In the current model structure gut absorption is handled with a two-compartment GI tract model developed for the CPF PBPK/PD model (Timchalk et al., 2002) which was based on the model structure used to describe the uptake of chlorinated solvents (Staats et al., 1991). It is well established that oral absorption of a chemical or drug can be modified by both intestinal and liver metabolism (Wacher et al., 2001; Zhang and Benet, 2001), modifying a chemical's bioavailability. A shift in the amount and rate of oral absorption could result in the observed alterations in the time-course of the parent compounds resulting in an increase and delay in achieving $C_{max}$. Poet et al. (2003) evaluated the *in vitro* intestinal (enterocytes) metabolism of both CPF and DZN and reported that intestinal CYP450 and PON-1 activity could impact the metabolism of CPF and DZN and subsequently modify *in vivo* bioavailability. Since enterocyte CYP450 activity is substantially lower than in liver, a dose-dependent saturation of the intestinal CYP450 based metabolism of CPF and DZN is feasible and could likewise contribute to greater bioavailability than would be encountered at lower doses. In this regard, ongoing model refinement is focused on the development of a more physiologically based description of the gut-compartment that incorporates relevant metabolic processes. Nonetheless, these results also suggest that at lower, more environmentally relevant doses, the kinetics of CPF and DZN would not be appreciably impacted by co-exposure to these insecticides.

For OP insecticides, the extent of ChE inhibition correlates with the amount of oxon formed, and the inhibitory potency ($K_i$) for the individual OP insecticides; since the oxon is directly responsible for the enzyme inhibition and inhibitory potency varies based on oxon binding affinities for ChE (Kousba et al., 2004). For CPF-oxon the apparent bimolecular inhibition rate constants ($K_i$) for AChE and BuChE were initially estimated by fitting experimental data (Timchalk et al., 2002); while for DZN-oxon, initial $K_i$ estimates for AChE and BuChE were based on the CPF-oxon data, and then optimized based on ChE inhibition data following *in vivo* DZN exposure (Poet et al., 2004). The parameter estimates for enzyme degradation ($K_d$) reactivation ($K_r$) and aging ($K_a$) for both CPF- and DZN-oxon were the same and were based on those determined for CPF-oxon (Timchalk et al., 2002), which is appropriate since both CPF-oxon and DZN-oxon share the same diethylphosphate group which phosphorylates the enzyme active site.

In general, the PBPK/PD model reasonably simulated the extent of RBC AChE and brain AChE inhibition for both CPF and DZN as single- or binary-exposures. Although the PBPK/PD model accurately simulated the extent of plasma ChE inhibition following either the CPF or CPF + DZN-binary-exposures at all dose levels, the model tended to under-estimate the DZN-only response at all dose-levels (See Fig. 6D–F). However, the model fit to the DZN-only plasma ChE response could be substantially improved by increasing the $K_i$ for BuChE (data not shown). Since rodent plasma ChE is the sum of both AChE and BuChE (50:50) and BuChE is more sensitive to the inhibitory effects of both CPF-oxon and DZN-oxon than is AChE (Amitai et al., 1998; Timchalk et al., 2002; Kousba et al.,

2003, 2007; Poet et al., 2004), improving the DZN fit by increasing the $K_i$ for DZN-oxon inhibition to the plasma ChE suggest that the current $K_i$ parameter estimate is underestimated.

The PBPK/PD model simulations were consistent with the published experimental data that demonstrate a clear dose- and time-dependent inhibition of brain, RBC, and plasma ChE activity and the extent of *in vivo* tissue sensitivity followed the order: plasma > RBC ≥ brain for both CPF and DZN and are quantitatively similar to previous findings with CPF and DZN in the rat (Timchalk et al., 2002; Poet et al., 2004). The greater ChE inhibition in the blood (plasma and RBC) relative to brain is partially explained by differences in dosimetry, since PBPK/PD model simulations predict substantially higher oxon AUCs (see Fig. 9) in the blood relative to the brain (Timchalk et al., 2002; Poet et al., 2004).

The overall potency for ChE inhibition was greater for CPF than DZN and the binary mixture response appeared to be strongly influenced by CPF at all doses (see Figs. 6–8). This is particularly interesting since the rats actually received slightly higher molar doses of DZN (∼14%; Timchalk et al., 2005), yet CPF was clearly more potent. This greater *in vivo* potency for CPF relative to DZN is consistent with the *in vitro* findings where the $V_{max_{app}}/K_{m_{app}}$ ratios for CYP450 metabolism of CPF → CPF-oxon and DZN → DZN-oxon were 6.7 and 1.5, respectively; which suggest that the metabolism of CPF to its oxon was ∼5× faster than for DZN. These findings are also consistent with a previous report by Poet et al. (2003); which also suggested that CPF was more rapidly metabolized to CPF-oxon relative to DZN. Additionally, it was previously reported that the rate of PON-1 detoxification for both CPF-oxon and DZN-oxon were similar. Based upon these comparisons the differences in CYP450 metabolic capacity may partially contribute to the observed differences in the *in vivo* ChE inhibition dynamics. Consistent with these conclusions are the model simulations of CPF- and DZN-oxon AUC in blood and brain (see Fig. 9). In the blood compartment the CPF-oxon AUC is ∼10× higher than for DZN-oxon (compare Fig. 9B and E); whereas, in the brain compartment the CPF-oxon AUC is ∼3× greater than for DZN-oxon. These *in vitro* results and the model simulations are consistent with the experimental observations (see Figs. 6–8) and support the importance that metabolism plays in differential toxicity to OP insecticides.

It is also possible that other reasonable mechanisms such as differences in the affinity of the oxon metabolites for ChE enzymes (including concentration-dependent interactions) or the depletion of important detoxification enzymes could contribute to observed differences in OP insecticide potency. In this current PBPK/PD model structure, the bimolecular inhibition rate constants for the interactions of CPF- and DZN-oxon with AChE, BuChE and CaE are primarily based on model optimizations against experimental ChE measurements (Timchalk et al., 2002; Poet et al., 2004). Although this approach has enabled a reasonable simulation of the experimental data sets, clearly further refinement and improvement of the model would be realized by experimentally determining these parameters. In this regard, recent studies suggest that the dynamics of OP interactions with AChE are both age- and concentration-dependent (Kousba et al., 2004, 2007; Kaushik et al., 2007). Kaushik et al. (2007) noted the importance of understanding the relationship between oxon concentrations at target sites following *in vivo* exposures versus the concentrations associated with changing *in vitro* $K_i$ values. In this regard, the ability to predict *in vivo* oxon concentrations with the PBPK/PD models may provide a quantitative approach for designing *in vitro* $K_i$ studies, and appropriate algorithms can then be developed to describe the dynamic changes in the apparent $K_i$ values as a function of tissue oxon concentration, as was recently done for a CPF age-dependent PBPK/PD model (Timchalk et al., 2007).

In assessing the strengths and weaknesses of the current modeling approach it is of particular importance to identify model weaknesses, since they offer the greatest opportunity for improvement. In the case of the current binary OP PBPK/PD model, with the exception of the previously published (Timchalk et al., 2005) experimental data used in the current manuscript, it is fully acknowledged that there is a dearth of *in vitro* or *in vivo* experimental data in rats and virtually no available human data for validation of this binary model. Secondly, at the high *in vivo* single- and binary-doses utilized in rats, clear signs of cholinergic toxicity were observed in most of the animals (Timchalk et al., 2005); yet, no attempt was made to modify the model to accommodate the changes in physiology (i.e. altered blood flow, cardiac output) that are clearly associated with cholinergic toxicity. The fact that blood flow to the brain was increased (3–7%) to more accurately reflect the extent of AChE inhibition may in part be partially associated with the observed neurotoxicity; however, alternative confounding factors cannot be excluded. For example Chambers and Chambers (1989) measured low levels of CYP450 desulfation metabolism of CPF in microsomes prepared from rat brains; indicating the potential for localized brain activation to CPF-oxon. In this regard, inclusion of brain CYP450 metabolism in the CPF PBPK/PD model does result in a reasonable fit of the brain AChE inhibition data while maintaining a 3% blood flow to the brain (data not shown). Although there is no experimental data supporting the brain CYP450 metabolism of DZN, the *in vitro* metabolism studies with CPF, CPF-methyl and leptophos (Chambers and Chambers, 1989) do suggest that further evaluation of the role of localized brain metabolism for the binary mixture may be useful. The results from the current study also point out the need for additional research to more fully ascertain the *in vivo* mechanism(s) for the observed binary metabolic interactions between CPF and DZN. In particular, additional studies are needed that focus on the early kinetics (<3 h post-dosing) to provide greater insight into the potential importance of intestinal first-pass metabolism for OP mixtures which will enable a more physiologically based description of gut-metabolism and absorption in the rat.

In conclusion, the binary PBPK/PD model reasonably describes the pharmacokinetic (dosimetry) and pharmacodynamic (ChE inhibition) impact of an acute oral binary-exposure to CPF and DZN in rats. It is anticipated that at low binary-doses,

most likely to be encountered in both occupational and environmental related exposures, the pharmacokinetics are expected to be linear. The current study also suggests that ChE inhibition kinetics are well described using a dose-additive model. This PBPK/PD binary OP model provides a mechanistic framework for understanding the lack of important synergistic interactions at occupationally and environmentally realistic exposures, even for pesticides that are as similar as CPF and DZN.

## Acknowledgements

This publication was partially supported by grants R01 OH003629 and R01 OH008173 from Centers for Disease Control and Prevention (CDC). Its contents are solely the responsibility of the authors and have not been subject to any review by CDC and therefore do not necessarily represent the official view of CDC, and no official endorsement should be inferred.

## References

Abu-Quare AW, Abdel-Rahman A, Brownie C, Kishk AM, Abou-Donia MB. Inhibition of cholinesterase enzymes following a single dermal dose of chlorpyrifos and methyl parathion, alone and in combination, in pregnant rats. J Toxicol Environ Health Part A 2001;63:173–89.

Amitai G, Moorad D, Adani R, Doctor BP. Inhibition of acetylcholinesterase and butyrylcholinesterase by chlorpyrifos-oxon. Biochem Pharmacol 1998;56:293–9.

Andersen ME, Gargas ML, Clewell HJ, Severyn KM. Quantitative evaluation of the metabolic interaction between trichloroethylene and 1,1-dichloroethylene *in vivo* using gas uptake methods. Toxicol Appl Pharmacol 1987;89:185–205.

Bradman A, Barr DB, Claus-Henn BG, Drumheller T, Curry C, Eskenazi B. Measurement of pesticides and other toxicants in amniotic fluid as a potential biomarker of prenatal exposure: a validation study. Environ Health Perspect 2003;111(14):1779–82.

Brown RP, Delp MD, Lindstedt SL, Rhomberg LR, Beliles RP. Physiological parameter values for physiologically based pharmacokinetic models. Toxicol Ind Health 1997;13:407–84.

Buratti FM, Volpe MT, Fabrizi L, Meneguz A, Vittozzi L, Testai E. Kinetic parameters of OPT pesticide desulfation by c-DNA expressed human CYPs. Environ Toxicol Pharmacol 2002;11:181–90.

Buratti FM, Volpe MT, Meneguz A, Vittozzi L, Testai E. CYP-specific bioactivation of four organophosphorothioate pesticides by human liver microsomes. Toxicol Appl Pharmacol 2003;186:143–54.

Calabrese EJ. Comparative metabolism: the principal causes of differential susceptibility to toxic and carcinogenic agents. In: Calabrese EJ, editor. Principles of animals extrapolation. Chelsea, MI: Lewis Publishers; 1991. p. 203–76.

Chambers JE, Carr RL, Boone S, Chambers HW. The metabolism of organophosphorus insecticides. In: Krieger R, Doull J, Ecobichon D, Gammon D, Hodgson E, Reiter L, Ross J, editors. Handbook of pesticide toxicology, vol. 2. San Diego: Academic Press; 2001. p. . p. 919–29.

Chambers JE, Chambers HW. Oxidative desulfuration of chlorpyrifos chlorpyrifos-methyl and leptophos by rat brain and liver 1989;4(3):201–3.

Chanda SM, Mortensen SR, Moser VC, Padilla S. Tissue-specific effects of chlorpyrifos on carboxylesterase and cholinesterase activity in adult rats: an in vitro and in vivo comparison. Fundam Appl Toxicol 1997;38:148–57.

Clement JG. Role of aliesterase in organophosphate poisoning. Fundam Appl Toxicol 1984;4:S96–105.

el-Masri HA, Reardon KF, Yang RS. Integrated approaches for the analysis of toxicologic interactions of chemical mixtures. Crit Rev Toxicol 1997;27(2):175–97.

Fabrizi L, Gemma S, Testai E, Vittozzi L. Identification of the cytochrome P450 isoenzymes involved in the metabolism of diazinon in the rat liver. J Biochem Mol Toxicol 1999;13(1):53–61.

FQPA (1996). Food Quality Protection Act, Public Law No. 104–170.

Gearhart JM, Jepson GW, Clewell HJ III, Andersen ME, Conolly RB. Physiologically based pharmacokinetic and pharmacodynamic model for the inhibition of acetylcholinesterase by diisopropylfluorophosphate. Toxicol Appl Pharmacol 1990;106:295–310.

Halpert J, Hammond D, Neal RA. Inactivation of purified rat liver cytochrome P-450 during the metabolism of parathion (diethyl *p*-nitrophenyl phosphorothionate). J Biol Chem 1980;255(3):1080–9.

Hayes AL, Wise RA, Weir FW. Assessment of occupational exposure to organophosphates in pest control operators. Am Ind Hyg Assoc J 1980;41(8):568–75.

Hodgson E, Rose RL. Organophosphorus chemicals: potent inhibitors of the human metabolism of steroid hormones and xenobiotics. Drug Metab Rev 2006;38(1–2):149–62.

Joo H, Choi K, Rose RL, Hodgson E. Inhibition of fipronil and nonane metabolism in human liver microsomes and human cytochrome P450 isoforms by chlorpyrifos. J Biochem Mol Toxicol 2007;21(2):76–80.

Karanth S, Liu J, Olivier K Jr, Pope C. Interactive toxicity of the organophosphorus insecticide chlorpyrifos and methyl chlorpyrifos in adult rats. Toxicol Appl Pharmacol 2004;196:183–90.

Karanth S, Olivier K Jr, Liu J, Pope C. *In vivo* interaction between chlorpyrifos and parathion in adult rats: sequence of administration can markedly influence toxic. Toxicol Appl Pharmacol 2001;177:247–55.

Kaushik R, Rosenfeld CA, Sultatos LG. Concentration-dependent interactions of the organophosphates chlorpyrifos oxon and methyl paraoxon with human recombinant acetylcholinesterase. Toxicol Sci 2007;221:243–50.

Kousba AA, Poet TS, Timchalk C. Age-related brain cholinesterase inhibition kinetics following in vitro incubation with chlorpyrifos-oxon and diazinon-oxon. Toxicol Sci 2007;95(1):147–55.

Kousba AA, Sultatos LG, Poet TS, Timchalk C. Comparison of chlorpyrifos-oxon and paraoxon acetylcholinesterase inhibition dynamics: potential role of a peripheral binding site. Toxicol Sci 2004;80:239–48.

Kousba A, Poet TS, Timchalk C. Characterization of the *in vitro* kinetic interaction of chlorpyrifos-oxon with rat salivary cholinesterase: a potential biomonitoring matrix. Toxicology 2003;188(2–3):219–32.

Krishnan K, Haddad S, Béliveau M, Tardif R. Physiological modeling and extrapolation of pharmacokinetic interactions from binary to more complex chemical mixtures. Environ Health Perspect 2002;110(Suppl. 6):989–94.

Lavy TL, Mattice JD, Massey JH, Skulman BW. Measurement of year-long exposure to tree nursery workers using multiple pesticides. Arch Environ Contam Toxicol 1993;24:123–44.

Lowe ER, Rick DL, West RJ, Bartels MJ. The evaluation of quantitative structure property relationship predictions of tissue–blood partition coefficients of high lipophilic chemicals. Drug Metab Rev 2006;38:78.

Lu C, Fenske RA, Simcox NJ, Kalman D. Pesticide exposure of children in agricultural community: evidence of household proximity to farmland and take home exposure pathways. Environ Res Sect A 2000;84:290–302.

Ma T, Chambers JE. Kinetic parameters of desulfuration and dearylation of parathion and chlorpyrifos by rat liver microcosms. Food Chem Toxicol 1994;32:763–7.

Ma T, Chambers JE. A kinetic analysis of hepatic microsomal activation of parathion and chlorpyrifos in control and phenobarbital-treated rats. J Biochem Toxicol 1995;10:63–8.

Marinovich M, Ghilardi F, Galli CL. Effect of pesticide mixtures on in vitro nervous cells: comparison with single pesticides. Toxicology 1996;108:201–6.

Maxwell DM, Lenz DE, Groff WA, Kaminskis A, Froehlich HL. The effect of blood flow and detoxification on *in vivo* cholinesterase inhibition by soman in rats. Toxicol Appl Pharmacol 1987;88:66–76.

Mileson BE, Chambers JE, Chen WL, Dettbarn W, Ehrich M, Eldefrawi AT, Gaylor DW, Hamernik K, Hodgson E, Karczmar AG, Padilla S, Pope CN, Richardson RJ, Saunders DR, Sheets LP, Sultatos LG, Wallace KB. Common mechanism of toxicity: a case study of organophosphorus pesticides. Toxicol Sci 1998;41:8–20.

Mortensen SR, Chanda SM, Hooper MJ, Padilla S. Maturational differences in chlorpyrifos-oxonase activity may contribute to age-related sensitivity to chlorpyrifos. J Biochem Toxicol 1996;11:279–87.

Moser VC, Casey M, Hamm A, Carter WH Jr, Simmons JE, Gennings C. Neurtoxicological and statistical analyses of a mixture of five organophosphorus pesticides using a ray design. Toxicol Sci 2005;86(1):101–15.

Moser VC, Simmons JE, Gennings C. Neurotoxicological interactions of a five-pesticide mixture in preweanling rats. Toxicol Sci 2006;92(1):235–45.

Mücke W, Alt KO, Esser HO. Degradation of $^{14}$C-labeled diazinon in the rat. J Agric Food Chem 1970;18:208–12.

Nolan RJ, Rick DL, Freshour NL, Saunders JH. Chlorpyrifos: pharmacokinetics in human volunteers. Toxicol Appl Pharmacol 1984;73:8–15.

Poet TS, Kousba AA, Dennison SL, Timchalk C. Physiologically based pharmacokinetic/pharmacodynamic model for the organophosphorus pesticide diazinon. NeuroToxicol 2004;25:1013–30.

Poet TS, Wu H, Kousba AA, Timchalk C. *In vitro* rat hepatic and enterocyte metabolism of the organophosphate pesticides chlorpyrifos and diazinon. Toxicol Sci 2003;72:193–200.

Poulin P, Krishnan K. An algorithm for predicting tissue:blood partition coefficients of organic chemicals from n-octonol: water partition coefficient data. J Toxicol Environ Health 1995;46:117–29.

Quandt SA, Arcury TA, Rao P, Snively BM, Camann DE, Doran AM, Yau AY, Hoppin JA, Jackson DS. Agricultural and residential pesticides in wipe samples from farmworker family residences in North Carolina and Virginia. Environ Health Perspect 2004;112(3):382–7.

Richardson JR, Chambers HW, Chambers JE. Analysis of the additivity of in vitro inhibition of cholinesterase by mixtures of chlorpyrifos-oxon and azinphos-methyl-oxon. Toxicol Appl Pharmacol 2001;172:128–39.

Sams C, Mason HJ, Rawbone R. Evidence for the activation of organophosphate pesticides by cytochromes P450 3A4 and 2D6 in human liver microcosms. Toxicol Lett 2000;116:217–21.

Staats DA, Fisher JW, Conolly RB. Gastrointestinal absorption of xenobiotics in physiologically based pharmacokinetic models. Drug Metab Dispos 1991;19:144–8.

Sultatos LG, Murphy SD. Kinetic analyses of the microsomal biotransformation of the phosphorothioate insecticides chlorpyrifos and parathion. Fundam Appl Toxicol 1983;3:16–21.

Tang J, Cao Y, Rose RL, Brimfield AA, Dai D, Goldstein JA, Hodgson E. Metabolism of chlorpyrifos by human cytochrome P450 isoforms and human, mouse, and rat liver microsomes. Drug Metab Dispos 2001;29(9):1201–4.

Timchalk C, Kousba AA, Poet TS. An age-dependent physiologically based pharmacokinetic/pharmacodynamic model for the organophosphorus insecticide chlorpyrifos in the preweanling rat. Toxicol Sci 2007;98(2):348–65.

Timchalk C, Poet TS, Hinman MN, Busby AL, Kousba AA. Pharmacokinetic and pharmacodynamic interaction for a binary mixture of chlorpyrifos and diazinon in the rat. Toxicol Appl Pharmacol 2005;205:31–42.

Timchalk C, Nolan RJ, Mendrala AL, Dittenber DA, Brzak KA, Mattsson JL. A physiologically based pharmacokinetic and pharmacodynamic (PBPK/PD) model for the organophosphate insecticide chlorpyrifos in rats and humans. Toxicol Sci 2002;66:34–53.

Wacher VJ, Salphati L, Benet LZ. Active secretion and enterocytic drug metabolism barriers to drug absorption. Adv Drug Deliv Rev 2001;46:89–102.

Yang RS, el-Masri HA, Thomas RS, Constan AA. The use of physiologically-based pharmacokinetic/pharmacodynamic dosimetry models for chemical mixtures. Toxicol Lett 1995;82–82:497–504.

Zhang Y, Benet LZ. The gut as a barrier to drug absorption combined role of cytochrome CYP 3A and *p*-glycoprotein. Clin Pharmacokinet 2001;40:159–68.